Journal of Green Engineering (JGE)

Volume-10, Issue-12, December 2020

SR-DCNN Based Paddy Leaves Disease Classification and Stages Identification

[1]K. Suresh, [2]S.Karthik, [3]M.Hanumanthappa

[1]Research Scholar, Research and Development Centre, Bharthiar University, Coimbatore, India. E-mail: mailsuresh.k@gmail.com
[2]Professor, S.N.S. College of Technology, Coimbatore, India. E-mail: profskarthik@gmail.com
[3]Professor, Bangalore University, Bangalore, India. E-mail:hanu6572@gmail.com

Abstract

In India, Paddy is the most imperative crops, and they are prone to numerous diseases, say, bacterial blight, rice blast, brown spot, et cetera. All the methodologies that were previously developed are less accurate and do not focus on detecting the stages. This paper proposed a paddy leaves disease classification and stages identification with the aid of SR-DCNN. This proposed method comprises totally '7' phases. Initially, the Image Acquisition (IA) process is carried out, and then, the ICLAHE enhances the contrast. Following the preprocessing, the CoK-means method clusters that image into disease affected leave and normal leaves. After that, the LoO method segment the disease affected part as of the disease leaves, and the features are extracted as of that segmented part. After Feature Extraction (FE), the features are selected utilizing the SAF-ACO algorithm. Then, these selected features are inputted to the SR-DCNN, which classifies the image as bacterial blight, rice blast, brown spot, leaf smut, and sheath blight. Lastly, the distance is gauged between the classified disease input of the images and query images utilizing Euclidean distance, which is employed to distinguish the disease's stages. In an experimental appraisal, the proposed work attains better accuracy than the prevailing methodologies.When contrasted to other classifiers, the proposed SR-DCNN classifier attains 98.95% accuracy in disease detection.

Keywords: Improved Contrast Limited Adaptive Histogram Equalization (ICLAHE), Covariance based K-means (COK-means), Logarithmic Otsu

Journal of Green Engineering, Vol. 10_12, 13276-13298.

Alpha Publishers

(LAO), Speed and Aggregation factor-Ant Colony Optimization (SAF-ACO) , Softmax and rectifier based Deep Convolutional Neural Network (SR-DCNN).

1 Introduction

In agriculture, rice plants face a critical issue due to diseases that lead to the degradation of the quality in addition to the quantity of the crops. This requires automatic plant disease recognition along with detection to ameliorate the yield [1]. In this nation, rice stands as the staple cereal crops; in addition, rice farming is regarded as the main agricultural economy [2]. Amid the rice growth, disparate diseases [3] that appear on rice plants are Leaf blast, Sheath blight, Brown spot, along with Leaf scald, etc. [4, 5]. Typically, these diseases extend from one spot to a disparate one by means of carrying agents, say, water, air, soil, insects, along with contaminated seeds [6]. Several diseases do not contain any observable indications, or the effect becomes perceptible too late to act, additionally in those circumstances, a complicated analysis is compulsory [7]. Although manual scrutiny can diagnose the disease, it becomes outmoded whilst taking into account big fields as well as non-native diseases. The naked eye scrutiny of specialists is the major approach that is adopted practically, which will be expensive for big farms.

Most farmers in rural regions ascertain disease physically, which might occasionally bring about a fault reorganization of the disease's type [8]. Image Processing (IP) methods assist in recognizing diseases more precisely as well as with-in a short time [9]. The methods that are concerned in the recognition of the paddy diseases are the IA, image preprocessing, image segmentation, FE, along with classification [10]. Disparate techniques were utilized for segmentation along with FE; in addition, for classification, disparate classifiers are present [11]. Usually, the Machine Learning (ML) algorithm is utilized to categorize the paddy leaves' disease, like artificial neural networks (ANN), supports vector machines (SVM), K-nearest neighbors (KNN) in addition to naive bayes, et cetera. After that, the imperative thing is stage classification that implies how much the diseases are pretentious.

Disease severity stands as the region (absolute or relative) of the sampling element (leaf) exhibiting disease symptoms [12]. The severity is calculated in ‘3’ disparate ways: i) Visual Rating, ii) Image Analysis, along with iii) Hyperspectral Imaging (HSI). Hyperspectral IP is turning out to be an active subject in Remote Sensing (RS) along with other applications in present times. HSI can simply differentiate resources, which are spectrally the same [13]. Recent sensor technologies are able to cover large surfaces of the earth with extraordinary spatial, spectral along with temporal resolutions. On account of these characters, HSIwas effectively utilized in copiousRS applications necessitating the assessment of the physical factor of numerous multifaceted exteriors [14].

Furthermore, HSI is an objective technique contrary to visual rating and also can be executed in an automatic system, resultant in a significantly lowered workload. This brings about a diminution of economic along with ecological cost in agricultural production [15]. A lot of researchers only concentrate on identifying the disease, but the enhancement is still required in the reorganization of the diseases' severity. If the disease is not detected at a previous phase itself, then it might bring about several yield loss. Thus, accurate detection is required. This document proposed a paddy leaves disease classification along with stages identification utilizing the HSI.

This paper is prearranged in the subsequentmeans: Section 2 renders the associated work. Section 3 briefly elucidates the proposed methodology. Section 4 renders the results together with the discussion of the proposed technique, and finally, in section 5, a conclusion has been drawn from the whole work.

2 Related Work

S. Ramesh and D. Vydeki [16] introduced the recognition along with the categorization of paddy leaves' diseases centered upon an optimized deep neural network with the jaya algorithm (DNN-JOA). Initially, in the IA, the rice plant leaves' images were taken directly as of the farm for normal, brown spot, bacterial blight, sheath rot, along with blast diseases. In preprocessing, for the background removal, the RGB images were transformed into Hue, saturation along with value (HSV) images. Centered upon the hue along with saturation sections, binary images were extracted to categories the i) diseased and ii) non-diseased parts. After that, a clustering technique was employed for the segmentation of the diseased, normal, together with background. Diseases' classification was carried out centered on a DNN-JOA. The experimental outcome illustrated that the technique attained enhanced performance than the prevailing technique.

Santanu Phadikar *et al.* [17] introduced rice disease classification centered on Feature Selection (FS) along with rule generation methods. Fermi energy-centered segmentation techniques were employed to separate the contaminated area of the image as of the background. Centered on the field specialist opinions, indications of the diseases were typified centered on features, such as color, shape, together with the position of the contaminated portion, and extracted by means of developing disparate algorithms. To decrease the classifier's complexity, significant features were chosen centered upon rough sets theory (RST) for reducing the loss of information. Lastly, centered on the chosen features, a rule-centered classifier had been constructed that enclosed every diseased rice plant images and also offered better outcome contrasted to the conventional classifiers

Basavaraj S. Anami *et al.* [18] introduced a categorization of yield that affected the biotic along with abiotics paddy crop stresses centered on-field images. The scheme comprised of '5' steps: IA, FE, FS, identification together with the categorization of paddy crop stresses. The scheme examined the stress responses with regard to the color differences centered on low-order color moments along with visual color descriptors. The Sequential Forwards Floating Selections were executed to lessen the overlapping amongst the features. The outcome illustrated that the scheme attained improved performance than the prevailing technique. However, the technique was intricate and also demanding with reference to higher irregularity in the outside environment.

Shampa Sengupta as well as Asit K. Das [19] suggested a particle swarms optimization centered incremental classifier for rice disease forecast. The incremental classifier was fitting to be implemented on the rice disease database for disease forecasting as the traits of rice diseases vary in time because of the alterations in climate, biological, along with geographical factors. The technique had been implemented on simulated rice disease datasets along with standard datasets; in addition, the classification accuracy was calculated as well as contrasted with disparate top-notch classification algorithms. The technique was also estimated centered on some statistical gauges along with that the statistical test was done to institute implication together with efficacy. The parameters utilized in incremental particles swarm optimization (IPSO) were experimentally set but the scheme insisted on a self-adapted parameter setting system.

Harshadkumar B. Prajapati*et al.* [20] introduced the discovery along with the categorization of rice plant diseases. The procedure of plant disease discovery was separated into '2' fractions, i) IP, ii) ML. The images were considered as of the farm field. These images were further progressed centered on IP; in the end, the ML categorized the diseases grounded on the image characteristics. To allow precise extraction of characteristics, the scheme utilized centroid feeding centered K-means clustering for segmentation of diseases portion as of a leaf image. The scheme improved the K-means clustering’s output by eliminating green pixels on the diseased part. The outcome illustrated that the scheme rendered improved performance than the prevailing technique.

Guoxiong Zhou *et al.* [21] recommended a rapid discovery of rice disease centered on the furry c-means-k means (FCM-KM). Initially, the technique utilized a ‘2’-dimensional filtering mask joined to a weighted multiple-level median filter aimed at noise diminution as well as utilized an earlier '2'-dimensional Otsu threshold segmentation to decrease the meddling of intricate background with the discovery of targeted blade on the image. After that, the dynamic populace firefly algorithm centered upon the chaos theory as well as the maximal and minimal distance algorithm was implemented for the optimization of the FCM-KM to ascertain the optimal clustering class k value. The outcome signified that the technique was additional competent to detect rice diseases.

Sánchez et al., [22] proposed an automated identification and classification method for Botrytis disease over machine-learning techniques such as SVM, ANN, random forest K-nearest neighbor algorithms. The proposed method uses various techniques they are morphological operations, Gaussian filter among others for the image feature extraction.

Qiang et al., [23] presented a GAN with dense fusion mechanisms and quadra residual and attention for the pest images low-resolution transformation. This method decreases the camera layout density in agricultural IOT monitoring scheme and infrastructure. In terms of classification, segmentation performance and visual quality, the proposed PSRGAN methods outperforms super resolution.

Vijai et al., [24] presents a various imaging techniques review for classification and detection of plant diseases. For plant disease classification this paper used computer vision approaches and the detection is started with image acquisition, pre-processing and segmentation. Further accompanied by feature extraction and classification.

3 Proposed Paddy Leaves Disease Classification And Stages Identification System Using SR-DCNN

Plants are one amongst the chief resources that could be utilized to shun global warming. Nevertheless, they are affected by Blast, Canker, Blackspot, Bacterial leaf Blights, Brown spot together with Cotton mold that hamper the growth in addition to productivity of plants, which in turn brings great economical and ecological losses. Thus, to shun such losses timely, it is better to diagnose them accurately and gauge the disease severity. This document proposed a paddy leaves disease classification and stages identification with the aid of SR-DCNN.

Fig. 1 illustrates the proposed paddy leaves disease classification and stages identification system. The proposed work encompassed by '7' stages they are i) Image Acquisition, ii) Pre-Processing, iii) Clustering, iv) Segmentation, v) Feature Extraction vi) Feature Selection, and vii) Classification. From the input image, image acquisition is performed which retrieves the original image form source followed by the pre-processing is executed. In this phase the ICLAHE ameliorates the image's contrast after that Covariance-centric k-means (CoK-means) clusters the images as the disease affected leaves and normal leaves then Logarithmic Otsu (LoO) segments the disease-affected leaves. Then the essential features are extracted as of that segmented part and the essential features are chosen by utilizing the SAF-ACO algorithm. And then, the SR-DCNN classifier takes those features (selected) as inputs. The SR-DCNN classifies the output as bacterial blight, rice blast, brown spot, leaf smut, in addition to sheath blight. Lastly, the distance is gauged between the classified disease input of the images and query images utilizing Euclidean distance (ED), which is utilized to identify the disease's stages.

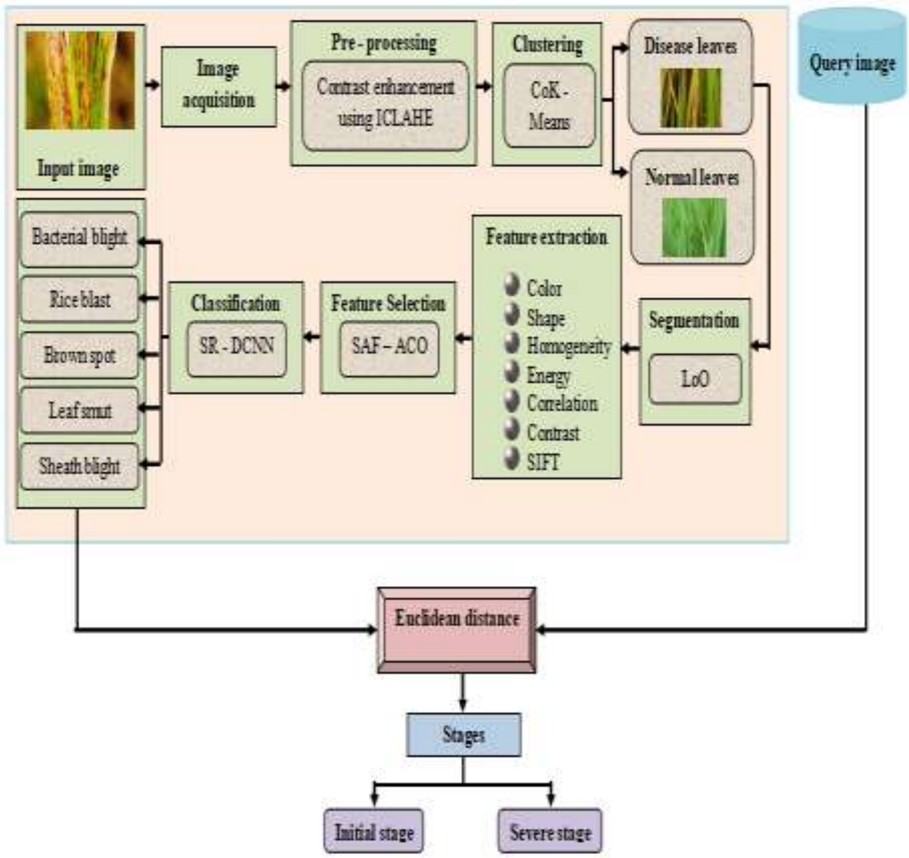

Figure 1 Block Diagram for the Proposed Methodology

3.1 Image Acquisition

IA is stated as the procedure of retrieval of an image as of some source in image processing. Here, the paddy leaves images are extracted as of the public depository. The dataset is mathematically indicated as,

$$P_D = \{p_1, p_2, ...p_n\} \quad (1)$$

Wherein, P_D implies the paddy leaf image dataset for additional processing and p_n signifies the n-number of leaf images in the dataset.

3.2 Preprocessing

Here, since the gathered images are tend to be of low quality, the preprocessing is executed. Furthermore, the proposed work employed the ICLAHE to acquire maximum accuracy.

3.2.1 Contrast Enhancement Using Iclahe

CLAHE differ as of standard histogram equalization in the terms that CLAHE functions on smaller regions in the image, termed tiles, and calculates numerous histograms, each in proportion to a distinct part of the image and utilize them to re-distribute, but in the intensity augmented in ICLAHE perform well. This algorithm is elucidated as,

Step 1: Read image

Take the entire inputted values that were employed in enhancement processes, say the number of regions in a Column and row direction individually, dynamic gamut (number of bins utilized in histogram transform function), distribution parameter type, clip limit.

Step 2: Convert image as of RGB (Red, Green, in addition to Blue) to HSI (Hue, Saturation, Intensities)

The RGB in addition to CMY color models is not suited for describing colors with respect to human interpretation. Color objects in images can be simply described by means of its saturation, hue, along with brightness (intensity). First, the Hue '**H**' is rendered by,

$$H = \begin{cases} \theta & if \;\; B \le G \\ 360 - \theta & if \;\; B > G \end{cases} \tag{2}$$

Where, $\theta = \cos^{-1}\left\{ \frac{1/2\left[(R-G)+(R-B)\right]}{\sqrt{\left[(R-G)^2+(R-B)(G-B)\right]}} \right.$ (3)

The saturation '**S**' is rendered by,

$$S = 1 - \frac{3}{(R+G+B)}[\min\,(R,G,B)] \tag{4}$$

The intensity 'I' are rendered by,

$$I = \frac{1}{3}(R+G+B) \tag{5}$$

All RGB values are normalized to the gamut [0,1].

Step 3: next, gauge the histogram of every contextual region as per gray levels that are present in the HSI image.

Step 4: computing the contrast limited histogram of the contextual area by clip limit value

In the contextual area, numbers of pixels are equally split in every gray level, thus, the average number of pixels $M^{''}_{n(p)}(I)$ is gray level, which is mathematically indicated as,

$$M^{''}_{n(p)}(I) = \frac{CR_{n(p)}(X) \times CR_{n(p)}(Y)}{CR_{n(g)}(l)} \tag{6}$$

Wherein, $CR_{n(p)}(X)$ signifies the number of pixels on the X direction of contextual region, $CR_{n(g)}(l)$ signifies the numbers of grey level in the contextual region and $CR_{n(p)}(Y)$ implies the numbers of pixels on the Y direction of the contextual region.

Step 5: Subsequently, compute the actual clip limit

$$A^{''}_{cl}(I) = N^{''}_{cl}(I) \times M^{''}_{n(p)}(I) \tag{7}$$

Wherein, $A^{''}_{cl}(I)$ signifies the actual clip limit and $N^{''}_{cl}(I)$ signifies the normalized clip limit in the range [0, 1].

Step 6: Grey level mapping is interpolated to generate an enhanced image. Here, use the four-pixel cluster and implement the mapping process, then every mapping-tile will partly overlap on the image region. Next, a single pixel will be extracted, and subsequently, employ '4' mappings to that pixel. Interpolate between that outcomes to get ameliorated pixels and repeat this over the entire image.

3.3 Clustering Using COK-Means

Subsequent to data pre-processing, the CoK-means clusters the normal and the disease affected leaves. The k-means clustering allots data points to the cluster in such wise it has minimal sum-of-squared-distance value between the clusters and the data points. Generally, this distance is computed by utilizing ED. The less variation inside a cluster, the more homogeneous (similar) the data points are inside that cluster. ED cohere when every dimension encompasses the same units (say meters) since it includes adding the squared value of them. However, it takes covariance in an account which aids in gauging the strength/similarity between '2' disparate data objects. Thus the term is termed CoK-means. This algorithm is elucidated as,

Step 1: Visualize n data points as well as settle on the number of clusters (k). And, k arbitrary points are picked as the centroids of each cluster.

Step 2: Next, gauge the distance of every point as of every cluster by gauging its distance as of the equivalent cluster mean as well as cluster centre,

$$Dist^{'}_{c} = \sum_{i=1}^{k} \sum_{j=1}^{k_i} \left(\| p_i - q_j \|^2 \right) * CV^{''}_{m} \tag{8}$$

Where, $CV^{''}_{m} = \sqrt{\left(p_i - q_j\right)^T M^{-1} \left(p_i - q_j\right)}$ (9)

Wherein, $\| p_i - q_j \|$ signifies the distance as of cluster centroid to the pixel of the image, $CV_m^{"}$ signifies the co-variance between the objects and M^{-1} signifies the covariance metrics.

Step 3: Allot every data point to an adjoining cluster (centroids).

Step 4: Gauge the centroids for the clusters by means of averaging the entire data points that be a member of every cluster.

Centered on the COK-means algorithm, the image is clustered into disease affected image $U_d^{"}(I)$ and disease non –affected image $U_{nd}^{"}(I)$.

3.4 Segmentation

Subsequent to clustering, the disease affected part is segmented as of the paddy leaves image utilizing LoO. Otsu's thresholdtechnique includes iterating via all the feasible threshold values as well as computing a gauge of spread for the pixel levels every side of the threshold, explicitly, the pixels that fall either in back-ground or fore-ground. In Otsu threshold, the normal mean calculation does not render the standard points. Thus, the logarithmic technique is employed to efficiently create the mean calculation. Therefore, the term is called LoO.

The algorithm is described in the below steps,

Step 1: Let the number of pixels at i gray level be b_i

Step 2: The likelihood of occurrence of the grey level i is stated as,

$$V_i^{"} = \frac{b_i}{B}, \quad V_i^{"} \geq 0, \quad \sum_{i=0}^{z} V_i^{"} = 1 \tag{10}$$

Wherein, $V_i^{"}$ signifies the cumulative moments of the grey level histogram and B signifies the number of the pixel at a provided image.

Step 3: $P_i^{"}(I)$ and $P_b^{"}(I)$ are normally equivalent to the object of interest and the background. Thus, the probabilities of the '2' classes are mathematically indicated in the below equation,

$$P_i^{"}(I) = \sum_{i=0}^{E} V_i^{"} \tag{11}$$

$$P_b^{"}(I) = 1 - P_i^{"}(I) \tag{12}$$

Step 4: The means of the classes $P_i^{"}(I)$ and $P_b^{"}(I)$ is calculated utilizing logarithmic calculation function,

$$\mu_{P_i^{"}(I)} = -\sum_{i=0}^{E} \frac{V_i^{"} \log V_i^{"}}{P_i^{"}(I)} \tag{13}$$

$$\mu_{P_b^{"}(I)} = -\sum_{i=0}^{E} \frac{V_i^{"} \log V_i^{"}}{P_b^{"}(I)} \tag{14}$$

Step 5: Its standard deviation ($\sigma^2(I)$) could be computed utilizing the equation (12) and (13)

$$\sigma^2(y) = P_i^{''}(I)\, P_b^{''}(I) \left(\mu_{P_i^{''}(I)} - \mu_{P_b^{''}(I)}\right)^2 \tag{15}$$

Step 6: **A**n optimal threshold $\sigma_{ot}^2(y^*)$ is ascertained by means of the discriminant criteria, which is to augment the separability of the ensuing classes in grey levels. This threshold technique is centered on choosing the lowest point between the '2' classes. Thus, the optimal threshold is ascertained by,

$$\sigma_{ot}^2(y^*) = \max \sigma^2(y) \tag{16}$$

Like this, the diseased part is segmented.

3.5 Feature Extraction

The vital features in the segmented disease part image are now extracted. In agriculture, numerous FE methods are extracted encompassing texture, color and shape, and every feature sort has its own challenges. In the proposed work, the SIFT (Scale Invariant Features Transform) features and shape, color, and textural features, say homogeneity, correlation, energy, and contrast, are extracted. Therefore, the features are elucidated as,

- ***Color feature***

These are more imperative since every disease encompasses its unique color, which is employed for recognition. It is extracted centered on the mean ($M_c^{''}(f)$) in addition to standard deviation ($SD_c^{''}(f)$), which is computed by utilizing the formula,

$$M_c^{''}(f) = \frac{1}{N}\sum_{i=1}^{n} H_{pq}^{''}(v) \tag{17}$$

$$SD_c^{''}(f) = \sqrt{\frac{1}{N}\sum_{i=1}^{n}\left(H_{pq}^{''}(v) - M_c^{''}(f)\right)^2} \tag{18}$$

Where,

N - Total number of pixels

$H_{pq}^{''}(v)$ - Pixel values

- ***Shape feature***

This one is as well an imperative feature for disease classification. It is computed centered on the area ($A_s^{''}(I)$) of the diseased portion as of the total region of the image, which is mathematically written as,

$$A_s^{''}(I) = \frac{D_p^{''}(I)}{T_a^{''}(I)} \tag{19}$$

Where,

$D_p^{"}(I)$ - Area of the diseased portion

$T_a^{"}(I)$ - Total area of an image

- ***Homogeneity (*** $H_p^{"}(f)$ ***)***

It might encompass a single or an assortment of values for ascertaining whether the image is textured or non-textured. It is mathematically signified as,

$$H_p^{"}(f)=\sum_{i=0}^{n}\frac{H_{pq}^{"}(v)}{1+(p-q)^2} \tag{20}$$

- ***Energy (*** $E_p^{"}(f)$ ***)***

The texture's uniformity is illustrated using this feature. Thus, the image's energy is higher when the image is extra homogeneous. There is an extremely tiny dominant gray-tone transition on the homogeneous image. It is signified as,

$$E_p^{"}(f)=\sum_{i=0}^{n}\left(H_{pq}^{"}(v)\right)^2 \tag{21}$$

- ***Correlation (*** $Cr_p^{"}(f)$ ***)***

It gauges the grey level linear dependence among pixels (relative to one another) at the particular positions; it encompasses high values when the values are distributed uniformly on the GLCM and low values if not. It is implied as,

$$Cr_p^{"}(f)=\sum_{i=0}^{n}H_{pq}^{"}(v)\ \frac{(p-M_c^{"}(f))(q-M_c^{"}(f))}{SD_c^{"}(f)} \tag{22}$$

- ***Contrast (*** $Ct_p^{"}(f)$ ***)***

It considered the distribution polarization of black and white pixels and illustrates the dynamic gamut of gray levels. It is calculated as,

$$Ct_p^{"}(f)=\sum_{i=0}^{n}H_{pq}^{"}\ (p-q)^2 \tag{23}$$

- ***SIFT Feature***

SIFT is employed for extracting key points and compute their descriptors. It is accountable for the recognition and description of the images' local features. SIFT computation comprises '4' phases of filtering operation: i) scale-space extrema detection (SSED), ii) finding keypoints, iii) orientation assignment to keypoints, iv) create keypoints descriptor. These phases are elucidated as,

- **SSED**

This phase is to identify the attained image Locations as well as scales that are attained by means of filtering the image. The image's scale-space is typified as a capacity $S^{"}_{(I)}(p,q,\sigma)$ that is delivered as of the convolution of a variable-scale Gaussian $V^{"}_{(G)}(p,q,\sigma)$ with an inputted image $I(p,q)$,

$$S^{"}_{(I)}(p,q,\sigma) = V^{"}_{(G)}(p,q,\sigma) * I(p,q) \tag{24}$$

Wherein,

$*$ -Convolution operation of the inputted image

- **Finding Keypoints**

This phase endeavors to distribute with some points as of the competitor rundown of key points by means of finding those that encompass a low difference or are insufficiently restricted on an edge. The assessment of the key points in the DoG pyramid at the extrema is rendered by,

$$E^{"}_{k}(z) = E + \frac{1}{2}\frac{\partial E^{-1}}{\partial z} z \tag{25}$$

Wherein $E^{"}_{k}(z)$ implies derivatives and E are attained at the sample point as well as z implies offset as of this point.

- **Orientation Assignment to Key Points**

This technique supposes a constant orientation to the key points in local image intensities with the entire image property.

- **Create Key Points Descriptor**

Here, every key points encompasses location, scale, as well as orientation. Every key points rotate the window to standard orientation.

Lastly, the extracted feature is mathematically written as,

$$F^{"}_{s} = \{F_1, F_2, F_3, ...F_k\} \tag{26}$$

Wherein, $F^{"}_{s}$ implies the feature set and signifies the k-number of features.

3.6 Feature Selection Using SAF-ACO

After FE, the necessary features are effectively selected with the aid of SAF-ACO algorithm. A swarm optimization strategy termed Ant colony optimization (ACO) is centered on ant behavior of seeking a way between its state and a food source. With enough computations, the ACO would always determine the optimum, but, as the search fully relies on random walks, a faster convergence could not be assured. But, the method utilizes the aggregation factor and speed to ascertain the best optimal solution and enhance the convergence time. Hence, it is named as SAF-ACO and is detailed in the succeeding steps,

Step 1: initially, create ants utilizing probabilistic transition rule, which is mathematically expressed as,

$$p_{cd}^{n}(k)=\begin{cases}\dfrac{[\tau_{cd}(k)]^{\alpha}\,.\,[\eta_{cd}]^{\beta}}{\sum_{l\in J_c^n}\left[\tau_{cl}(k)^{\alpha}\,.\,[\eta_{cl}]^{\beta}\right]} & if \quad d\in D_c^n\\ 0 & otherwise\end{cases} \qquad (27)$$

Here,

n - Number of ants,

η_{cd} - Heuristic desirability of selecting feature d at node c

J_c^n - Set of neighbor nodes of node c which those "n"ants not visited yet

$\tau_{cd}(k)$ - Quantity of the virtual pheromone on edge (c,d).

$\alpha>0$ and $\beta>0$ - '2' parameters that ascertain the relative significances of the heuristic information and pheromone value.

Step 2: Contrarily, set the numbers of ants to be located on a graph equivalent to the number of existing features in the data. Every ant builds path at a disparate feature. As of those initial positions, the ants probabilistically traverse edges till the traversal stopping condition is highly satisfied. But, rather than traversing all the edges, the proposed method ascertains the optimal way by utilizing aggregation factor and speed, and then the pheromone on all edges are updated by utilizing the equation (28),

$$\tau_{cd}(k+1)=(1-\rho)\,.\,\tau_{cd}(k)+\rho.\sum_{n=1}^{i}\left(\gamma^{'}\left(S^{n}\right)/\,|\,S^{n}\,|\right)\times f^{"}(s)\times f^{"}(a) \qquad (28)$$

Where, $$f^{"}(s)=\frac{F\left(O_c^{"}(k)\right)}{F\left(O_l^{"}(k-1)\right)} \qquad (29)$$

$$f^{"}(a)=\frac{F\left(O_c^{"}(k)\right)}{M_b^{"}(n)} \qquad (30)$$

Wherein, ρ implies pheromone evaporation parameter that decays the pheromone trail, S^{n} signifies the feature sub-set found by ant n, $f^{"}(s)$ implies the speed factor and $f^{"}(a)$ signifies the aggregation factor. Now, update the pheromone as per both the gauge of the "goodness" of the ant's feature sub-set $\gamma^{'}$ and the sub-set's size. By this statement, all ants update the pheromone. In this way, the features are chosen as of the above extracted features, and these chosen ones have the denotation of,

$$S^{'}(F_s^{"})=\{F_1,F_2,F_3,......................F_n \qquad (31)$$

Wherein, $S^{'}\left(F_s^{"}\right)$ implies the selected feature set.

3.7 Classification Using SR-DCNN

Subsequent to FS, the chosen features are inputted to the SR-DCNN. A typical Convolutional Neural Network (DCNN) architecture encompasses convolution, connected, pooling, fully, and softmax-and-rectifier (SR) layers. The DCNN classifier involves more number of layers. Short description of those layers is elucidated as,

3.7.1 Convolution Layer (CL)

The initial layer which extracts features as of an inputted image is called CL. In the feature maps (FMs), the neurons are prearranged and each one has a corresponding receptive field. This field is linked to neighbor neurons of the preceding layer via trainable weights called filter-bank.

3.7.2 Pooling Layer (PL)

The PL integrates semantically related features onto a single feature, while the CL learns features. It independently operates on every FM. It lessens the spatial resolution of the FMs, and hence, attains spatial invariance to input distortions as well as translations. Its each unit takes input as of the units of the preceding layer and outputs an average or maximum of those values.

3.7.3 Fully-connected Layer (FCL)

Every unit in this FCL is linked to all the existent units of the preceding layer. It takes the output of CL/PL and predicts the best label for describing the image.

3.7.4 Softmax Layer and Rectifier Layer

The softmax transforms all the net activations of the final output layer simply to a series of values that could be interpreted as probabilities, whereas, the rectifier lets the network to converge too quickly.

The SR-DCNN could be detailed using its structure shown as Figure 2,

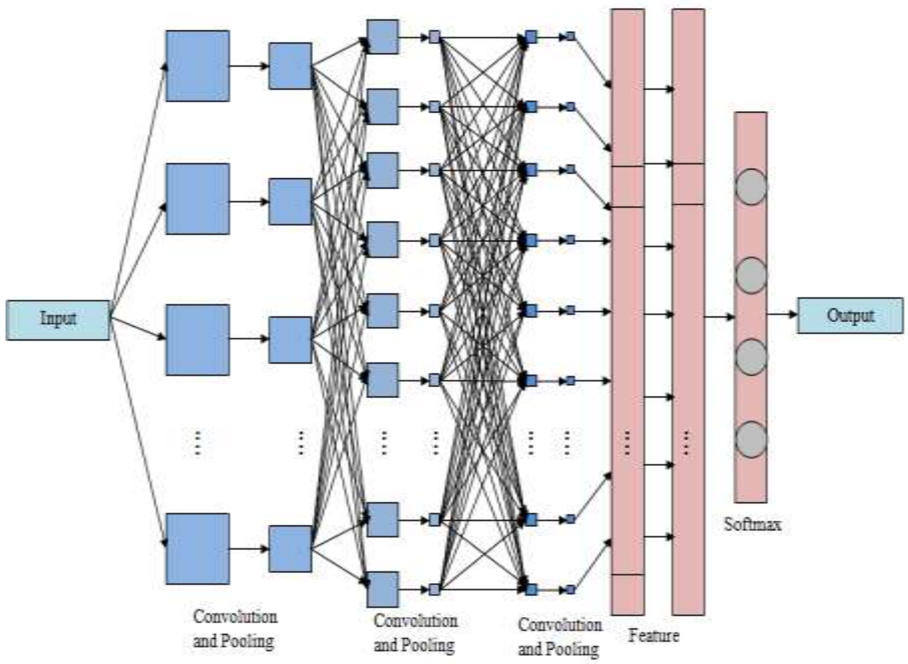

Figure 2 Structure of SR-DCNN

The feed-forward network called Convolutional neural network (CNN) extract features as of the inputted images or Feature Maps ($F_m^{"}$). Each CNN layer could have innumerable convolution kernels, which are utilized to attain multiple FMs. In the computation of the activation value AV_c^l of convolutional feature, $NL_a(.)$ indicate the non-linear activation function, which is proffered as:

$$AV_c^l = NL_a\left(F_m^{"}\right) \tag{32}$$

The Pooling Layer (PL_a^f) lessens the FM dimensions and maintains the scale invariance of the features moderately. Each FM of a PL is linked to its corresponding FM of the preceding CL. The pooling functions are symbolized as $p_f^{"}(.)$ for each FM and the PL_a^f is evaluated as:

$$PL_a^f = p_f^{"}\left(AV_c^l\right) \tag{33}$$

Max pooling and Average pooling indicates typical pooling operations.

After several CL and PLs, there may be at least one FCL. Once the image is passed via many CLs and PLs, numerous image maps are attained. The FCLs integrates all the attained image maps to get the high-layer semantic features of the image for performing subsequent image classification. The FCL function is symbolized as $f_c^{"}(l)$ and it creates global semantic information as of the preceding layer. Lastly, the softmax activation function is utilized for evaluating the final output and is expressed as,

$$SM_f^i = \frac{f_c^{''}(l) + bias}{R(f)} \tag{34}$$

Where,

SM_f^i - Final softmax output,

$R(f)$ -Weight value of the layer

$bias$ -Bias value

Here, $R(f)$ is given centered on the rectifier equation and is evaluated as,

$$R(f) = \max(0, x) * w_v^{'} \tag{35}$$

Where, $w_v^{'}$ signifies the weight value. If the function gets a negative input, it returns 0, but if any positive value" x " it returns it back. This function could back propagate the errors easily and contains multiple neurons layers which are activated by the rectifier function. Lastly, this classifier categorizes the images as a) Bacterial blights $B_d^l(I)$, b) rice blast $R_d^l(I)$, c) brown spot $Br_d^l(I)$, d) leaf smut $L_d^l(I)$, and e) sheath blight $S_d^l(I)$.

The proposed SR-DCNN's pseudo-code could be detailed using Fig 3,

---

Input: $S^{'}(F_s^{''}) = \{F_1, F_2, F_3, ...F_n$

Output: Bacterial blight $B_d^i(I)$, rice blast $R_d^i(I)$, brown spot $Br_d^i(I)$, leaf smut $L_d^i(I)$ and sheath blight $S_d^i(I)$

Begin

Initialize $AV_c^i, PL_a^f, f_c^{''}(l)$ and SM_f^i

Calculate the number of training samples

Numfeature=n //image features

if (numfeature) = 0

error (numfeature not integer);

end if

for $f_c^{''}(l)$ **do**

Calculate activation function by using,

$$SM_f^i = \frac{f_c^{''}(l) + bias}{R(f)} \quad // \textit{softmax activation}$$

for each features **do**

Convolution feature map using $AV_c^i = NL_a(F_m^{''})$

Max-pooling feature map using $PL_a^f = p_f^{*}(AV_c^i)$

end for

end for

End

Figure 3 Pseudo code for the SR-DCNN

After classification, the distance is gauged between the classified disease input of the images and query images utilizing ED as,

$$Dist_e^{"}(a,b) = \sqrt{(a_i - b_i)^2} \tag{36}$$

Where, $i = 1,2,3,.......n$ and a and b signifies the classified disease input image and query image. Grounded on this computation, the stages are detected, which means a certain threshold is fixed by this proposed approach. If the Euclidean output is below that threshold, then it signifies the primary stage. Otherwise, the stage is concerned as a severe stage.

4 Results and Discussion

Here, the proposed paddy leaves disease classification and identification of stages' performance is analyzed. The system is executed in MATLAB.

4.1 Performance Analysis

The proposed SR-DCNN's performance is estimated and contrasted with that of the existing classifiers say existing DCNN, CNN, together with ANN. The performance comparison is performed by computing accuracy, recall, precision, F-measure, specificity, sensitivity, False Discovery Rates (FDR), along with False Positive Rates (FPR).

Table 1 Demonstrate the Performance of the Proposed SR-DCNN and the Existing Methods.

Metrics	Proposed SR-DCNN	DCNN	CNN	ANN
Accuracy	98.95	93.38	92.15	90.72
Sensitivity	96.78	32.05	91.21	90.02
Specificity	95.63	91.42	90.34	89.13
Precision	96.98	92.99	91.67	90.47
Recall	94	90.03	89.04	87.74
F-measure	93.99	91.13	90.37	88.32
FDR	0.09	0.41	0.62	0.78
FPR	0.013	0.25	0.29	0.31

Table 1 compared the SR-DCNN's performance with the DCNN, CNN, along with ANN. The performance is estimated centered on the metrics, like precision, accuracy, f-measure, FDR, recall, along with FPR. As of the table, the ANN offers lower-level performance. Additionally, the existing DCNN and CNN show low-level performance than the proposed SR-DCNN. Thus, the proposed SR-DCNN is established to encompass high-level performance than the prevailing scheme. This is graphically signified from Figure 4,

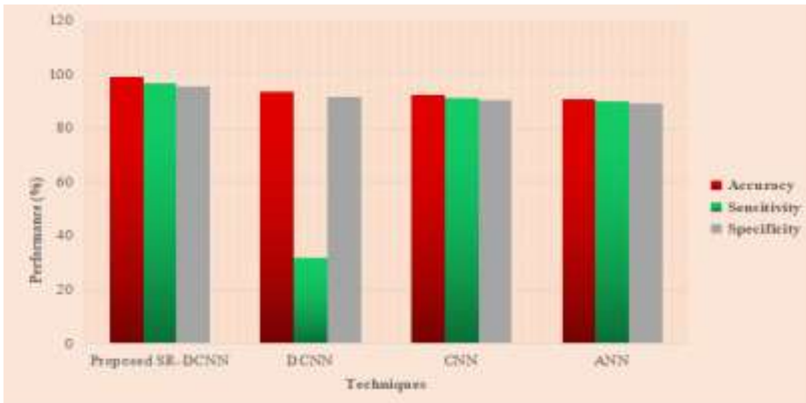

Figure 4 Accuracy, Sensitivity and Specificity Graph for Proposed and Existing Techniques

Figure 4 contrasts the proposed SR-DCNN's performance with that of the CNN, DCNN, along with ANN concerning the accuracy, sensitivity, together with specificity. As of the figure, the proposed SR-DCNN attains 98.95 % accuracy but the DCNN, CNN, along with ANN have 93.38 %, 92.15 % as well as 90.72 % accuracy, which is low when contrasted to the proposed one. Likewise, the proposed SR-DCNN has 96.78 % sensitivity along with 95.63 % specificity. However, the DCNN, CNN, along with ANN have a sensitivity value of 92.05 %, 91.21 % along with 90.02 % as well as the specificity value of 91.42 %, 90.34 % along with 89.13 %, which is lesser than the proposed work. Therefore, it deduces that the proposed SR-DCNN renders higher-level performance than the prevailing system.

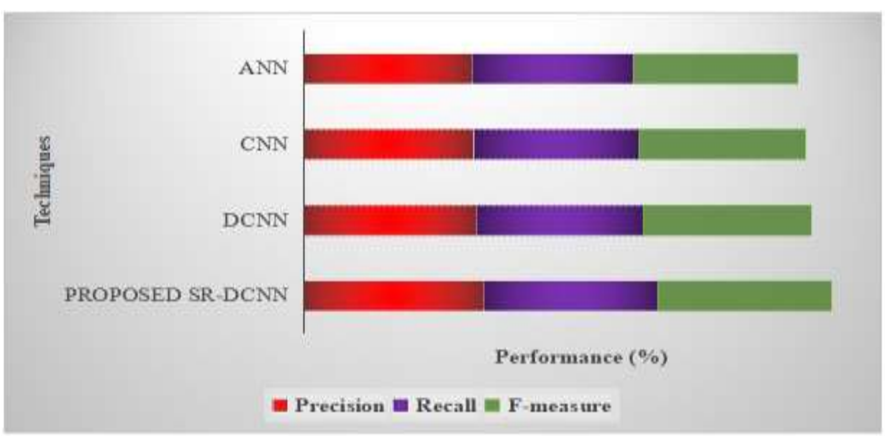

Figure 5 Comparative Analysis of the Proposed SR-DCNN with the Existing DCNN, CNN, and ANN.

Figure 5 showed that the SR-DCNN's performance with that of the DCNN, CNN, along with ANN-centered upon precision, recall, along with f-measure. Precision along with recall makes it potential to access the classifier's performance on the minority class. These amounts are associated to the harmonic mean of recall along with precision, which is an f-measure. As of the figure, the ANN offer lower-level performance, which encompasses 90.47% precision, 87.74 % recall along with 88.32 % f-measure, however, the proposed one attains 96.98 % precision, 94 % recall along with 93.99 % f-measure. Thus, it is defined that the SR-DCNN offers an improved outcome for all stated measures than the prevailing classifiers.

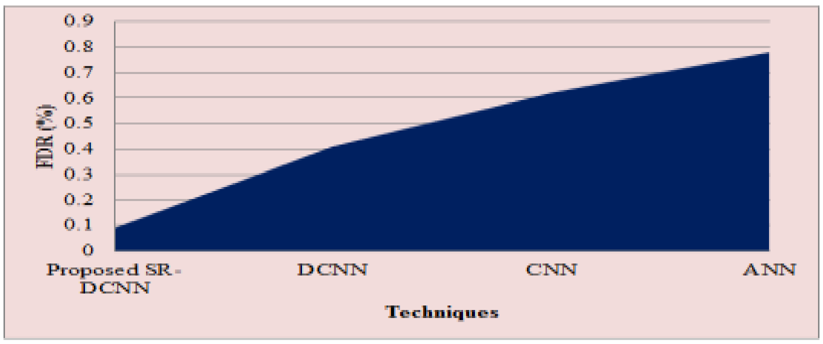

Figure 6 Performance of FDR with Respect to a Number of Techniques

Figure 6 exhibits the proposed SR-DCNN's performance with that of the DCNN, CNN, along with ANN. The FDR stands as the ratio of the number of false-positive outcomes to that of the total positive test outcomes. If the FDR value is low than 5 %, then the scheme is considered a good scheme. As of the figure, the proposed attains 0.09 % FDR, but the DCNN, CNN, along with ANN contains 0.44 %, 0.62 % along with 0.78 % FDR, which is high than the proposed SR-DCNN. So, the proposed work offers improved performance than the prevailing techniques.

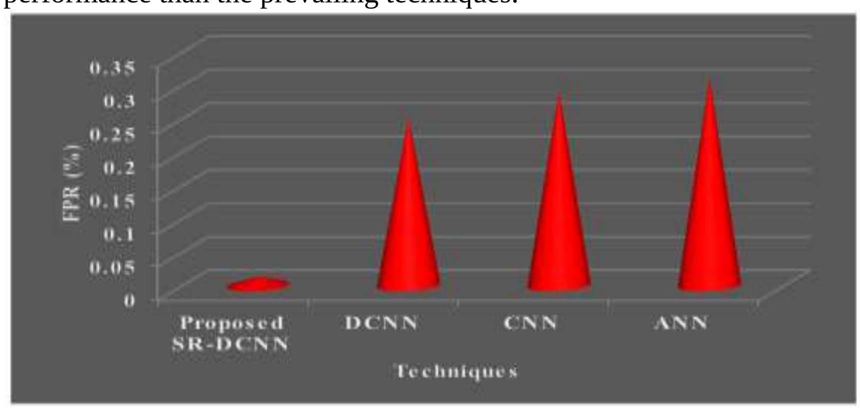

Figure 7 False Positive Rate Graph for Proposed and Existing Methods

Figure 7 illustrates the proposed SR-DCNN's performance with that of theDCNN, CNN, along with ANN. The performance is contrasted centered on the FPR. While statistically doing manifold comparisons, an FPR is the likelihood of incorrectly refusing the null hypothesis for a specific test. It typically refers to the expectation of the FPR. If the scheme has the greatest FPR value, the scheme is regarded as a good system. The proposed SR-DCNN has 0.013 % FPR, which is high when compared to the prevailing classifiers. As of the figure, it is obviously illustrated that the SR-DCNN classifier is improved than the prevailing scheme.

5 Conclusion

The paddy leaves disease classification and stages identification is performed here using SR-DCNN. The accurate detection of disease stages in paddy leaves is a notable process for preserving the paddies (rice plants). For this, the proposed work encompasses phases like IA, preprocessing, clustering, segmentation, FE, FS, together with classification. A disparate novel algorithm was utilized in those phases for the accurate disease stages identification. The proposed SR-DCNN classifier and the existing DCNN, CNN, and ANN classifiers are contrasted centered on their performance in respect of sensitivity, accuracy, precision, specificity, recall, f-measure, FDR, and FPR. When contrasted to other classifiers, the proposed SR-DCNN classifier attains 98.95% accuracy in disease detection. Hence, the proposed system is proved to have excellent results in paddy leaves disease classification and stages identification. This proposed work could be enhanced In the future by detecting other major diseases utilizing advanced algorithms.

References

[1] A.D. Nidhis, Chandrapati Naga Venkata Pardhu, K. Charishma Reddy, K. Deepa, "Cluster based paddy leaf disease detection, classification and diagnosis in crop health monitoring unit", Computer Aided Intervention and Diagnostics in Clinical and Medical Images, Springer, Cham, Vol. 31, pp. 281-291, 2019.

[2] S. Ramesh, "Rice blast disease detection and classification using machine learning algorithm", 2nd International Conference on Micro-Electronics and Telecommunication Engineering (ICMETE), IEEE, Ghaziabad, India, pp. 255-259, 2018.

[3] K. Sukhvir, P. Shreelekha, G. Shivani, "Plants disease identification and classification through leaf images: A survey", Archives of Computational Methods in Engineering, Vol. 26, No. 2, pp. 507-530, 2019.

[4] P. Jitesh Shah, B. Harshadkumar. Prajapati, K. Vipul Dabhi, "A survey on detection and classification of rice plant diseases", IEEE International Conference on Current Trends in Advanced Computing (ICCTAC), IEEE, Bangalore, India, pp. 1-8. 2016.

[5] Y. Ghazaala, K. Asit Das, A. Ghosal, “A hierarchical stratagem for rice leaf disease distinction”, In International Conference on Intelligent Computing, Instrumentation and Control Technologies (ICICICT), IEEE,Kannur, India, pp. 1177-1183, 2017.
[6] M. Suresha, K.N. Shreekanth, B.V. Thirumalesh., “Recognition of diseases in paddy leaves using knn classifier”, 2nd International Conference for Convergence in Technology (I2CT), IEEE, Mumbai, India, pp. 663-666, 2017.
[7] Srdjan Sladojevic, Marko Arsenovic, Andras Anderla, Dubravko Culibrk, Darko Stefanovic, “Deep neural networks based recognition of plant diseases by leaf image classification”, Computational intelligence and neuroscience, 2016.
[8] Farhana Tazmim Pinki, Nipa Khatun, SM Mohidul Islam, “Content based paddy leaf disease recognition and remedy prediction using support vector machine”, 20th International Conference of Computer and Information Technology (ICCIT), IEEE, Dhaka, Bangladesh, pp. 1-5. 2017.
[9] Taohidul Islam, Manish Sah, Sudipto Baral, Rudra RoyChoudhury, “A faster technique on rice disease detectionusing image processing of affected area in agro-field”, Second International Conference on Inventive Communication and Computational Technologies (ICICCT), IEEE, Coimbatore, India, pp. 62-66, 2018.
[10] R.P. Narmadha, G. Arulvadivu, “Detection and measurement of paddy leaf disease symptoms using image processing”, International Conference on Computer Communication and Informatics (ICCCI), IEEE,Coimbatore, India, pp. 1-4. 2017.
[11] A. Amrita Joshi, B.D. Jadhav, “Monitoring and controlling rice diseases using Image processing techniques”, International Conference on Computing, Analytics and Security Trends (CAST), IEEE,Pune, India, pp. 471-476, 2016.
[12] Johanna Albetis, Sylvie Duthoit, Fabio Guttler, Anne Jacquin, Michel Goulard, Hervé Poilvé, Jean-Baptiste Féret, Gérard Dedieu, “Detection of Flavescence dorée grapevine disease using unmanned aerial vehicle (UAV) multispectral imagery”, Remote Sensing, Vol. 9, No. 4, pp. 308, 2017.
[13] Savita Sabale P. and Chhaya R. Jadhav, “Hyperspectral image classification methods in remote sensing-a review”, International Conference on Computing Communication Control and Automation, IEEE,Pune, India, pp. 679-683, 2015.
[14] Muhammad Jaleed Khan, Hamid Saeed Khan, Adeel Yousaf, Khurram Khurshid, and Asad Abbas, “Modern trends in hyperspectral image analysis: A review”, IEEE Access, Vol. 6, pp. 14118-14129, 2018.
[15] Stefan Thomas, Matheus Thomas Kuska, David Bohnenkamp, Anna Brugger, Elias Alisaac, Mirwaes Wahabzada, Jan Behmann, and Anne-Katrin Mahlein, “Benefits of hyperspectral imaging for plant disease detection and plant protection: a technical perspective”, Journal of Plant Diseases and Protection, Vol. 125, No. 1, pp. 5-20, 2018.

[16]S. Ramesh, D. Vydeki, “Recognition and classification of paddy leaf diseases using Optimized Deep Neural network with Jaya algorithm”, Information Processing in Agriculture, Vol. 7, No. 2, pp. 249--260, 2019.
[17]Santan Phadikar, Jaya Sil, Asit Kumar Das, “Rice diseases classification using feature selection and rule generation techniques”, Computers and electronics in agriculture, Vol. 90, pp. 76-85, 2013.
[18]Basavaraj Anami, S., Naveen N. Malvade, and Surendra Palaiah, “Classification of yield affecting biotic and abiotic paddy crop stresses using field images”, Information Processing in Agriculture, Vol. 7, No. 2, pp. 272-285, 2020.
[19]S. Shampa, and K. Asit Das, “Particle swarm optimization based incremental classifier design for rice disease prediction”, Computers and Electronics in Agriculture, Vol. 140, pp. 443-451, 2017.
[20]B. Harshadkumar Prajapati, P. Jitesh Shah, and K. Vipul Dabhi, “Detection and classification of rice plant diseases”, Intelligent Decision Technologies, Vol. 11, No. 3, pp. 357-373, 2017.
[21]Z. Guoxiong, Z. Wenzhuo, C. Aibin, H. Mingfang, M. Xueshuo, “Rapid detection of rice disease based on FCM-KM and faster R-CNN fusion”, IEEE Access, vol. 7, pp. 143190-143206, 2019.
[22]M.G. Sánchez, V. Miramontes-Varo., J.A Chocoteco., V. Vidal, “Identification and Classification of Botrytis Disease in Pomegranate with Machine Learning” Advances in Intelligent Systems and Computing, Springer, Cham, Vol. 1229, 2020.
[23]D. Qiang, C. Xi, Q. Yan, Z. Youhua, Agricultural Pest Super-Resolution and Identification with Attention Enhanced Residual and Dense Fusion Generative and Adversarial Network, IEEE Access, Vol. 8, pp. 81943-81959, 2020.
[24]S. Vijai, S. Namita, S. Shikha, A review of imaging techniques for plant disease detection, Artificial Intelligence in Agriculture, Vol. 4, pp. 229-242, 2020.

Biographies

Suresh K working as a Professor in the Department of Computer science at Sindhi College, Bangalore, Karnataka. He has 12 years teaching experience.He has published one research paper in National journal.

S.Karthik is currently serving as Dean and Professor in the Department of Computer Science and Engineering at SNS college of Technology, Coimbatore. He has been in this line for many years with many awards and recognitions to his credit.He has authored many research papers and delivered talks in many forums.

Hanumanthappa M is working as a Professor & Chariman, Department of Computer Science & Applications, Bangalore University, Banglore. He has vast teaching and industry experience spreading over two decades at postgraduate level and various IT industries. He has authored more than 100 research papers in reputed International Joiurnals and peer reviewed Conference papers at International and National levels. He is the receipt of the best paper publication award by many organizations. His research interest includes Data Mining, Informaiton Retrieval, Network Security and Natural Language Processing. He is the Chairman for the Board of Studies in Computer Science of Bangalore University, Tumkur University, Bangalore North University and Bangalore Central University. He is the Board of Studies member in Computer Science for the various Universities across the country.